

Charge Transport Properties in Dye-Sensitized Nanostructured TiO₂ Thin Film Electrodes Studied by Photoinduced Current Transients

Anita Solbrand, Anders Henningsson,[†] Sven Södergren,[†] Henrik Lindström, Anders Hagfeldt,* and Sten-Eric Lindquist*

Department of Physical Chemistry, Uppsala University, P.O. Box 532, S-751 21 Uppsala, Sweden, and Department of Physics, Uppsala University P.O. Box 530, S-751 21 Uppsala, Sweden

Received: May 6, 1998; In Final Form: October 27, 1998

The charge transport in dye-sensitized nanostructured TiO₂ was studied by laser pulse induced photocurrent transients. The experimental curves were compared to simulations using a diffusion model with an initial electron distribution of an exponential decay. The simulations were optimized with respect to the experimental curves giving an apparent diffusion coefficient of 6×10^{-6} cm²/s for the electrons with an electrolyte of 0.1 M KI in propylene carbonate, the potential being +300 mV vs Ag/AgCl in ethanol. The charge transport was highly dependent on electrolyte composition and light intensity.

Introduction

Dye-sensitized nanostructured TiO₂ is a promising material for solar cell applications¹ since it is expected to be produced at a relatively low cost and can give efficiencies of up to 10%.^{1–3} A good understanding of the charge transport in the nanostructured material is of great importance for the development of a more efficient cell.

The charge transport in TiO₂ has been described by diffusion^{4,5} and diffusion coefficients for the electron in nanostructured TiO₂ has been estimated ranging from 1×10^{-2} to 1×10^{-7} cm²/s.^{6,7} The diffusion coefficient of the I₃[−] ion in the nanoporous network of TiO₂ has been determined to 7.6×10^{-6} and 3.2×10^{-6} cm²/s.¹¹ The solvents were acetonitrile/3-methyl-2-oxazolidinone (50:50 wt %) and acetonitrile, respectively. We have reported a value of 1.5×10^{-5} cm²/s for the diffusion of electrons in nanostructured TiO₂ with a supporting electrolyte of 0.7 M LiClO₄ in ethanol.⁵ The diffusion coefficient is in the same order of magnitude as the diffusion of ions in the electrolyte. The highest reported value, 1×10^{-2} cm²/s,^{6,7} was for electrons diffusing inside one colloidal particle; i.e., the electron did not pass any grain boundaries. Cao et al., who reported the lowest value, 1×10^{-7} cm²/s, of the diffusion coefficient, used a solid electrolyte where we used a liquid. It is obvious from this short review of experimental results that the charge transport in nanostructured materials are system dependent; i.e., it depends not only on the properties of the nanostructured material, e.g. its chemical structure and morphology, but also on the properties of the electrolyte in the pores. The transport of the electrons in the conduction band of e.g. TiO₂ or ZnO is inherently coupled to the charge transport of ions in the solution. The screening of the electrons in the nanostructured material by the electrolyte has been discussed by several authors.^{12,13}

Different mechanisms for the charge transport have been discussed, e.g. tunneling through potential barriers between the particles^{13,14} and a trapping/detrapping mechanism.^{15–19} These mechanisms are all random walk processes and cannot always be separated out from the measurements.

In this paper the charge transport has been studied with time-resolved photocurrents induced by laser pulses.^{20,21} The excitation has been with monochromatic light of lower photon energy than the band gap energy of TiO₂ in order to ensure that only electrons injected from the dye contributes to the photocurrent. The charge transport has been studied as a function of film thickness with illumination both from electrolyte/electrode (EE) and the substrate/electrode (SE) interface side.²² Also the dependence of electrolyte, light intensity and potential have been investigated and simulations of a diffusion model were carried out.

Theoretical Approach

The charge transport in nanostructured TiO₂ has in previous papers been described by diffusion.^{4,5} The time-dependent diffusion equation

$$\frac{\partial n(x,t)}{\partial t} = D \frac{\partial^2 n(x,t)}{\partial x^2} \quad (1)$$

where D is the chemical diffusion coefficient for the electron coupled to its image charge, x is distance from the back contact, t is time, and n is electron concentration, was solved for electrons with an initial delta-distribution. The delta-distribution was located at the outermost layer of the nanostructured TiO₂ thin film electrode representing an electron distribution created by absorption of a laser pulse in a very narrow section of the electrode. These electrons are assumed to diffuse toward the back contact where they are collected as a photocurrent transient. A laser pulse is used in order to ensure a negligible time for the creation of the initial distribution.⁵

In dye-sensitized electrodes, the light can be absorbed by both the TiO₂ and the dye, giving charge separation both in the TiO₂ and in the dye from where the electron is injected into the TiO₂. If the wavelength of the light is chosen longer than the onset for the absorption in the TiO₂, there will only be excitation in the dye followed by electron injection. This gives an initial distribution of the electrons in the film dependent upon the optical density of the dye, i.e., the amount of dye and its

* Authors to whom correspondence should be addressed.

[†] Department of Physics.

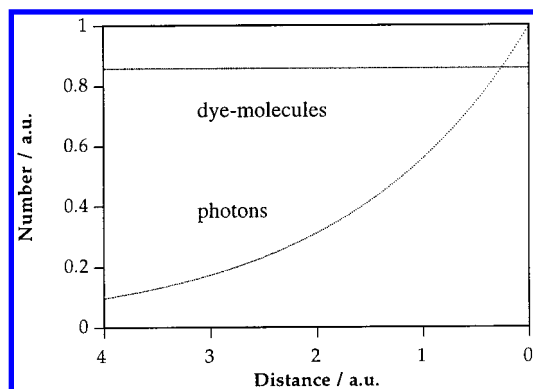


Figure 1. The number of photons and dye molecules in arbitrary units vs distance from the back contact for a 4.1 μm thick electrode.

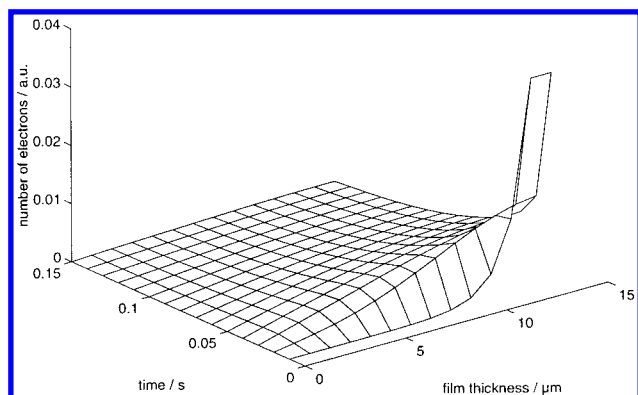


Figure 2. The number of photons vs distance from the back contact at various times after a laser pulse. The apparent diffusion coefficient was $6 \times 10^{-6} \text{ cm}^2/\text{s}$.

absorption coefficient. Here it is assumed that the absorption of light follows Lambert–Beers law, i.e., an exponential decay of the intensity along the direction of the propagation of the light. Hence, the initial distribution will have the shape of an exponential decay. If the light intensity is high enough, there will also be a considerable bleaching. This is probably the case in some of the experiments described in the present paper, especially for the thinner electrodes. For the thinnest electrode (4.1 μm), the amount of dye is estimated to be approximately twice as high as the number of photons in one laser pulse. This gives the absorption profile displayed in Figure 1 where the created electron distribution should have the shape of a truncated exponential function.

The time-dependent diffusion equation was solved numerically with a finite difference method with steps of 0.1 ms (∂t) and 1 μm (∂x). The boundary conditions were chosen as a truncated exponential decay for the initial distribution of the electrons. It is assumed that the electrons are reflected at the surface of the electrode and if the electrons reach the back contact they are removed, i.e., withdrawn as current. The stability of the calculations were tested to ensure that the errors did not grow. The electron distribution at different times after the laser pulse is shown in Figure 2. The electrons are withdrawn at the back contact, $x = 0$, as a photocurrent and a plot of the photocurrent vs time for the calculation above is displayed in Figure 3. These are the same conditions as for the photocurrent transients for the 12.8 μm thick electrode illuminated from the EE side (see Results and Discussion). The diffusion coefficient was obtained by optimizing the time for the second current peak in the simulated curve with respect to the experiment with an iterative process. No corrections for losses were made in the simulations.

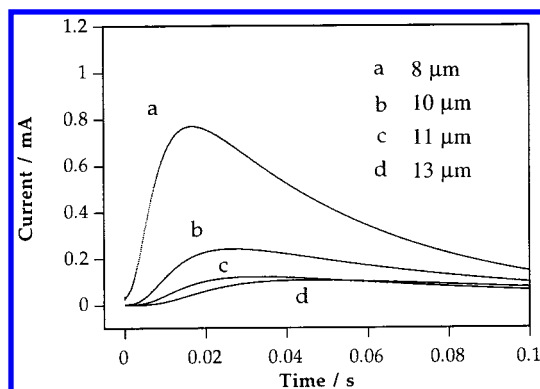


Figure 3. Current vs time calculated for four different thicknesses which are reported in the graph. The apparent diffusion coefficient was $6 \times 10^{-6} \text{ cm}^2/\text{s}$.

The mechanism of the charge transport is not discussed in detail here, but we will argue for a trapping/detrapping mechanism^{13,15,16} since some of the experimental results in this paper as well as earlier results²³ point in this direction. A trapping/detrapping mechanism implies that sub bandgap energy states are involved in the charge transport giving different time constants for the random walk process of the diffusion.¹⁵ This effect will be more pronounced the higher the density of trap states is and the lower the amount of electrons is. This will result in a number of diffusion coefficients for the electron transport, i.e., the diffusion coefficient obtained from the experimental results is only an apparent diffusion coefficient.

In the experimental curves there is a first transient with a decay in the millisecond time regime that is visible in all EE measurements, except for the thinnest electrode, which has not been accounted for in these simulations. It has earlier been explained as a capacitive effect and could just be added to the current transients as

$$I_{\text{RC}} = (q'/\tau)e^{-t/\tau} \quad (2)$$

where I_{RC} is the current arising from an RC circuit, q' is the charge affected at the back contact, and τ is the time constant of the RC circuit.⁵

Experimental Section

Electrode Preparation and Characterization. The electrode preparation has been described in detail elsewhere.²⁴ In short, a colloidal solution of TiO₂ was prepared by acidic hydrolysis of titanium isopropoxide and autoclaving at 200 °C, giving a colloidal radius of approximately 7 nm. The thin film electrodes were prepared by spreading the colloidal suspension onto conducting glass sheets (Libbey Owens Ford (LOF), fluorine-doped SnO₂ glass, sheet resistance 8 Ω/square) using Scotch tape as a frame and spacer, and raking off the excess solution with a glass rod. Different thicknesses were achieved by repeating the procedure 1–4 times. The electrodes were sintered in 450 °C in air for 30 min after each application. After the last sintering, while the electrodes still were hot they were immersed into the dye bath consisting of 0.5 mM ruthenium dye, *cis*-bis-(thiocyanato)bis(2,2'-bipyridyl-4,4'-dicarboxylate)ruthenium-(II) (Solaronix), in ethanol. The electrodes were left to soak in the dye bath for at least 24 h to ensure a homogeneous coloration. It is important to note that the prepared TiO₂ films are highly transparent, making the assumption that the absorption of light for a dye-sensitized film follows the Lambert–Beer law reasonable.

The electrode thicknesses were measured with a Tencor Alpha Step profilometer with an accuracy of $\pm 0.1 \mu\text{m}$. The illuminated area of the electrode is used for area compensating when necessary. The absorbance of all dyed electrodes were measured before and after exposure to the laser pulses and a small bleaching (less than 5%) of the electrodes was noticed after approximately 100 laser pulses. No spectral changes were observed. The thinnest electrode had an absorbance of 1.0 absorbance units and the thicker had absorbances of 2 and higher at 460 nm. No corrections were made for reflections and light scattering. The amount of dye on the electrodes was approximated using earlier dye desorption measurements.²⁵

Spectroelectrochemical Cell and Apparatus. The cell was a conventional three-electrode setup, consisting of a quartz cuvette with a Ag/AgCl reference electrode in ethanol and a platinum counter electrode. The dye-sensitized nanostructured TiO_2 thin film electrode was the working electrode. Used as light source was a single shot excimer laser (ELI-94, Estonian Academy of Science) pumping a dye laser (LT-1113, ELTO) giving 460 nm with a pulse duration of 30 ns. The laser pulse was defocused to approximately 1 cm^2 of homogeneously illuminated area and the intensity was measured before and after each set of measurements, using a joulemeter (Molelectron, JD 100). The transients are only directly comparable if the intensity is constant during the measurements since there is a high intensity dependence which is shown in Figure 11. This is the case within each set of measurements but not between the different sets. The working electrode was held at +300 mV vs Ag/AgCl in ethanol unless otherwise reported. The potentiostat was EG&G Princeton Applied Research, model 273, with a rise time of less than $10 \mu\text{s}$.⁵ The current transients were recorded using a digital oscilloscope (Hewlett-Packard 54600A, 100 MHz, $1 \text{ M}\Omega$). Each transient reported is an average of eight measurements recorded with at least 20 s intervals to ensure good reproducibility; i.e., the transients were allowed to decline completely before the next measurement. When the measurements were performed on different electrodes with different film thicknesses, each transient was normalized with respect to the electrode area. All measurements were performed under nitrogen atmosphere and in the dark, since the indoor light gives a positive background current. A small deterioration of the dye, less than 10%, was observed when the measurements were performed in oxygen atmosphere. The quantum yield was approximately 10% in all measurements. No corrections were made for reflections in the glass.

Chemicals. All chemicals used were of at least reagent grade. The electrolytes were prepared from water-free propylene carbonate (Aldrich) and water-free KI (Merck). As an inert salt, lithium trifluoromethanesulfonate (Aldrich) was used. All electrolytes were transparent at 460 nm.

Results and Discussion

The transients were studied varying the film thickness, electrolyte, working electrode potential, and the light intensity. The results will be described and discussed below.

Film Thickness. Photocurrent transients were measured for five different film thicknesses. Illumination was performed both from the electrode/electrolyte interface side (EE) and from the substrate/electrode interface side (SE). These measurements are reported in Figures 4A and 5, respectively. The electrolyte was 0.1M KI in propylene carbonate. When the electrode is illuminated in the EE direction, the thinnest electrode gives the highest photocurrent and the fastest transient, which is expected since the electrons have the shortest distance to travel to the

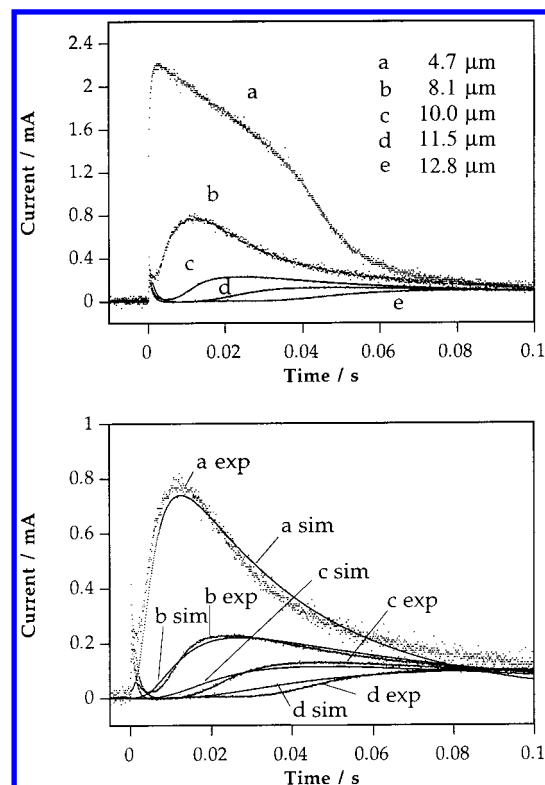


Figure 4. (A, top) Photocurrent vs time for five different film thicknesses which are reported in the graph with illumination direction EE. The electrolyte was 0.1 M KI in propylene carbonate and the potential was +300 mV vs Ag/AgCl in ethanol. (B) Simulated and experimental current transients for the four thicker films where the apparent diffusion coefficient have been optimized for each thickness and is (a) $8.1 \mu\text{m}$ with $D = 8 \times 10^{-6} \text{ cm}^2/\text{s}$, (b) $10.0 \mu\text{m}$ with $D = 6 \times 10^{-6} \text{ cm}^2/\text{s}$, (c) $11.5 \mu\text{m}$ with $D = 5 \times 10^{-6} \text{ cm}^2/\text{s}$, and (d) $12.8 \mu\text{m}$ with $D = 3 \times 10^{-6} \text{ cm}^2/\text{s}$.

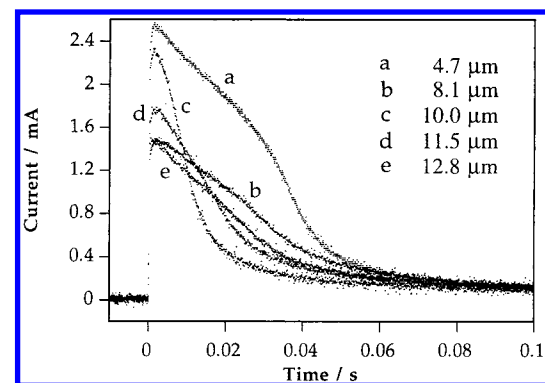


Figure 5. Photocurrent vs time for five different film thicknesses which are reported in the graph with illumination direction SE. Experimental conditions were the same as in Figure 4.

back contact. The shape of the transient for the thinnest electrode differs from the other transients and this could be due to a high degree of bleaching compared to thicker electrodes giving a larger amount of electrons created close to the back contact and hence a different initial distribution. When the electrode is illuminated from the SE side (see Figure 5), the behavior is different and not so systematic. The thinnest electrode still gives the highest photocurrent but the other films do not give photocurrents systematically changing with their thicknesses. If the films are not homogeneous all the way to the back contact, the amount of dye close to the back contact can vary and hence give a different absorption profile. Here the initial distribution of excited electrons is located close to the back contact in all

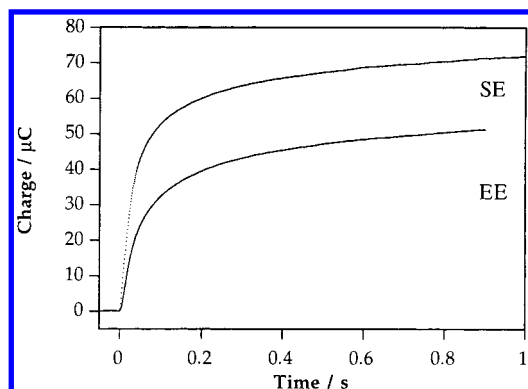


Figure 6. Charge vs time for a 8.1 μm thick electrode with experimental conditions as in Figure 4.

films; i.e., the exponential function has its maximum at the back contact and decays toward the surface of the electrode. This gives that the difference in the initial distribution will have a larger effect on the SE measurements since the differences will be smoothed out by the diffusion process for the EE measurements, especially for thicker films. Some electrons will diffuse toward the surface of the electrode, and if they are not lost to the electrolyte on their way, they will be reflected at the surface and diffuse back to the back contact. Thus these electrons have a longer transport distance and a higher probability of being lost to electron scavenging species in the electrolyte. Thinner films have a higher probability for the electrons to return to the back contact if reflected and should hence give a higher amount of charge collected.

The total amount of charge collected is highest for the thinnest electrode, 4.1 μm , both in the EE and in the SE measurements. In the EE measurements, the total amount of charge collected is decreasing with increasing film thickness but in the SE measurements there is no systematic trend for the four thicker films. For each electrode the collected charge is higher when the illumination is SE than if it is EE, except for the thinnest electrode where the amount of charge is independent of illumination direction. This indicates that the thickness of the film is in the range of the diffusion length.⁴ This could also influence the shape of the transients for the thinnest electrode. The charge vs time for EE and SE illumination for a 8.1 μm thick electrode is shown in Figure 6. The difference in collected charge between SE and EE illumination increases with film thickness, showing losses during the transport of the electrons to the back contact. This has also been observed in steady state measurements.²²

The current transients were fitted to the simulated curves described earlier giving an apparent diffusion coefficient of $6 \times 10^{-6} \text{ cm}^2/\text{s}$ (see Figure 3). This value is of the same order as the diffusion coefficient for the I_3^- ion.^{10,11} For unsensitized TiO₂ the apparent diffusion coefficient was determined to $1.5 \times 10^{-5} \text{ cm}^2/\text{s}$ in 0.7 M LiClO₄ in ethanol. Comparing the simulations with the experimental results, see Figures 3 and 4a, shows a deviation at thicker films. The experimental transients are delayed compared to the simulated curves, which can be explained by losses to the electrolyte or trapping.²³ Thicker films give a higher total amount of traps and hence a larger fraction of electrons being trapped/detrapped, and a longer time for the electron transport gives a larger probability for the electron to be lost to the electrolyte. This could also be discussed as a change in the apparent diffusion coefficient and if the simulated transient for each thickness is optimized with respect to the experiments the following apparent diffusion coefficients are obtained, $D = 8 \times 10^{-6} \text{ cm}^2/\text{s}$ for 8.1 μm , $D = 6 \times 10^{-6}$

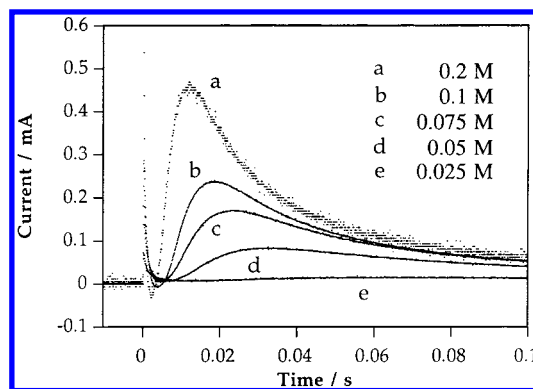


Figure 7. Photocurrent vs time for a 10.0 μm thick electrode at +300 mV vs Ag/AgCl in ethanol with illumination direction EE. The electrolyte was KI in propylene carbonate; the concentrations are given in the graph.

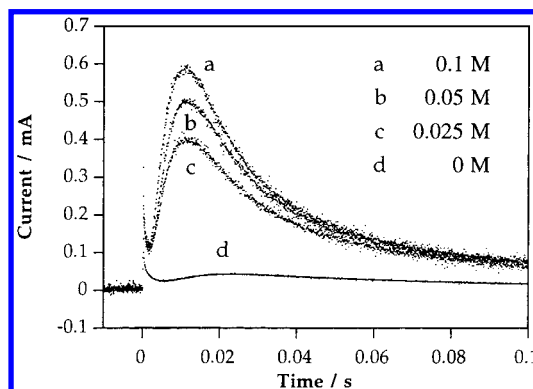


Figure 8. Photocurrent vs time for a 10.0 μm thick electrode at +300 mV vs Ag/AgCl in ethanol with illumination direction EE. The electrolyte was 0.1 M KI in propylene carbonate plus different concentrations of lithium trifluoromethanesulfonate which are reported in the graph.

cm^2/s for 10.0 μm , $D = 5 \times 10^{-6} \text{ cm}^2/\text{s}$ for 11.5 μm , and $D = 3 \times 10^{-6} \text{ cm}^2/\text{s}$ for 12.8 μm . Both the simulated and experimental curves are shown in Figure 4b.

Electrolyte. Current transients were recorded for a 10.0 μm thick electrode in electrolytes consisting of KI in propylene carbonate of different concentrations which are shown in Figure 7. All measurements were performed with EE illumination. The highest concentration gives the highest photocurrent and it decreases with decreasing concentration. Also the total amount of collected charge decreases with decreasing electrolyte concentration. The iodide is used to reduce the oxidized dye, and in the solar cell the efficiency is for this reason expected to be dependent upon the concentration of iodide.⁷ The KI can also contribute to the charge transport in the nanostructured TiO₂ by facilitating the charge compensation of the electrons in the electrode as was shown earlier.^{5,23} The transients were simulated for the different concentrations giving apparent diffusion coefficients varying from $3 \times 10^{-6} \text{ cm}^2/\text{s}$ (0.05 M) to $9 \times 10^{-6} \text{ cm}^2/\text{s}$ (0.2 M) showing the dependence on the charge transport of the electrolyte.

An inert salt, lithium trifluoromethanesulfonate (LTS), was added to a 0.1 M KI in propylene carbonate electrolyte and the photocurrent transients were measured; see Figure 8. The concentration of KI was held constant. The photocurrent increased drastically when 0.025 M LTS was added. The increase was not as pronounced when the concentration was changed to 0.05 or 0.1 M LTS though it continued to increase with concentration. The same trends were observed for the total amount of collected charge. This shows that an inert salt also

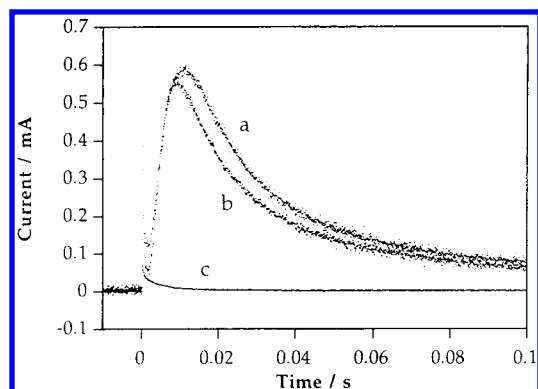


Figure 9. Photocurrent vs time for a 10.0 μm thick electrode at +300 mV vs Ag/AgCl in ethanol with illumination direction EE. The electrolyte was (a) 0.2 M KI, (b) 0.1 M KI + 0.1 M lithium trifluoromethanesulfonate, and (c) 0.2 M lithium trifluoromethanesulfonate.

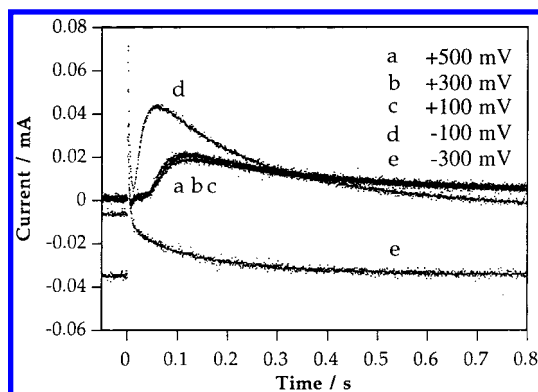


Figure 10. Photocurrent vs time for a 10.0 μm thick electrode in 0.1 M KI in propylene carbonate with illumination direction EE. The potentials reported in the graph are vs Ag/AgCl in ethanol.

affects the charge transport in the nanostructured electrodes. This is probably due to surface adsorption of the Li^{+26} giving a high amount of positive charge at the surface and hence a higher charge compensation of the electrons in the TiO_2 .

The photocurrent transients were measured in electrolytes consisting of 0.2 M KI, 0.1 M KI + 0.1 M LTS, or 0.2 M LTS for a 8.1 μm thick electrode which is shown in Figure 9. When there is no iodide present the current is mainly the initial capacitive current even though the concentration of inert salt is high. The inert salt increases the current compared to the electrolyte with only iodide; see also Figure 7. Thus there is a cooperative effect between reduction of the dye and conductivity of the electrolyte. The same observations were made for the total amount of collected charge for these three electrolytes.

Potential. Photocurrents were recorded in a potential interval of +500 mV to -300 mV vs Ag/AgCl in ethanol. The electrode thickness was 10.0 μm , the electrolyte 0.1 M KI in propylene carbonate and the illumination direction EE. The results are displayed in Figure 10. Similar transients were recorded at +100, +300, and +500 mV, although a small positive background current is observed at +500 mV. When the potential is shifted to -100 mV there is a negative background current and the photocurrent maximum increases. The transient also becomes faster. This is probably because the traps are already filled and there are free electrons in the conduction band at the moment of the laser pulse and hence the electron transport is facilitated. At -300 mV the negative background current is quite large and the positive maximum of the transient has disappeared. The electrode was irreversibly damaged by lowering the potential to -500 mV. At +300 mV where most of the measurements

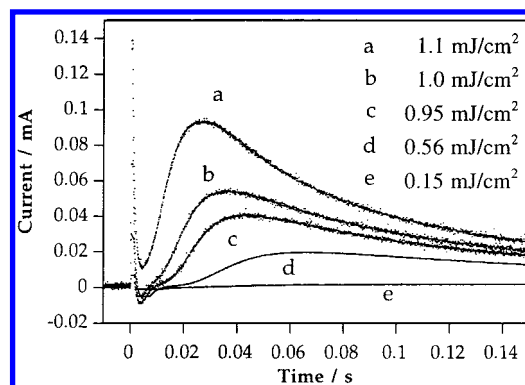


Figure 11. Photocurrent vs time for a 10.0 μm thick electrode in 0.1 M KI in propylene carbonate at +300 mV vs Ag/AgCl in ethanol. The light intensities are reported in the graph.

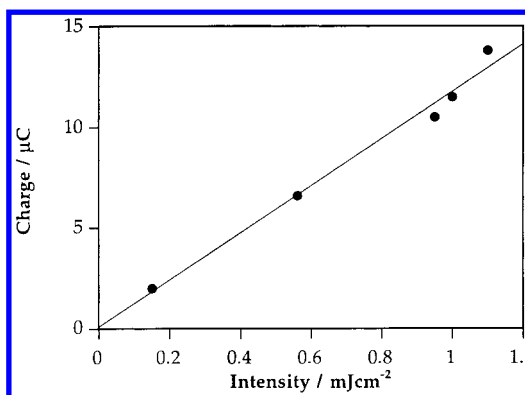


Figure 12. Charge vs intensity for the measurements reported in Figure 11.

were performed there is a plateau of high photocurrent and negligible dark currents/background currents are observed. The nanostructured TiO_2 electrode is not as dependent on potential as nanostructured ZnO .¹³ One possible explanation is if the amount of traps is higher in ZnO than in TiO_2 .

Light Intensity. The photocurrent transients were recorded at different light intensities (EE) for a 10.0 μm thick electrode in 0.1 M KI in propylene carbonate and are shown in Figure 11. The current amplitude decreases with decreasing light intensity as expected. The time for the current maximum increases with decreasing intensity which could be due to filling of traps as for ZnO ;^{13,23} i.e., the number of traps are the same but the lower light intensity gives a smaller number of excited electrons and this gives a larger fraction of the electrons used to fill the traps. If the total amount of collected charge is plotted vs the light intensity, it gives a straight line passing through the origin, indicating that the charge is directly proportional to the light intensity; i.e., there are no intensity-dependent losses. The quantum yield is at all intensities about 12% with no corrections for reflections in the glass.

Conclusions

The charge transport in dye-sensitized nanostructured TiO_2 can be described by diffusion and an apparent diffusion coefficient for the electrons can be calculated to be in the range $(3-8) \times 10^{-6} \text{ cm}^2/\text{s}$ at +300 mV in 0.1 M KI in propylene carbonate by optimizing the simulated transients with respect to the experimental curves. The laser pulse induced distribution of excited electrons is described by an exponential decay due to the absorption of the dye and therefore the diffusion equation was solved numerically for this case. The values of the apparent

diffusion constants correspond good with previous results on unsensitized TiO₂.⁵ There are losses during the transport to the back contact giving the highest quantum yield for the thinnest electrode, 4.1 μm , both for EE and SE illumination.

The charge transport is highly dependent on the electrolyte composition. A high amount of I⁻ gives a high photocurrent and addition of an inert salt raises the photocurrent amplitude, though there is almost no photocurrent with only inert salt.

The intensity affects the time for the current transients but not the quantum yield. This can be explained by trapping/detrapping as has been done earlier.^{13,15,23}

The charge transport is not dependent upon the potential in the range +500 to +100 mV. At lower potentials there is a negative dark current and at very low potentials an irreversible degradation of the electrodes is observed.

The diffusion model describes the major features of the charge transport but to make it complete it should be modeled with the trapping/detrapping mechanism included.

Acknowledgment. We thank Dr. Håkan Rensmo for stimulating discussions and Dr. Jan Alsins for helping us with the laser. This work has been supported by the Swedish Research Council for Engineering Sciences (TFR), the Swedish Natural Science Research Council (NFR), and the comission of the European Community Joule III program.

References and Notes

- (1) O'Regan, B.; Grätzel, M. *Nature* **1991**, 353, 737–740.
- (2) Hagfeldt, A.; Grätzel, M. *Chem. Rev.* **1995**, 95, 49–68.
- (3) Hagfeldt, A.; Didriksson, B.; Palmquist, T.; Lindström, H.; Södergren, S.; Rensmo, H.; Lindquist, S.-E. *Sol. Energy Mater. Sol. Cells* **1994**, 31, 481.
- (4) Södergren, S.; Hagfeldt, A.; Olsson, J.; Lindquist, S.-E. *J. Phys. Chem.* **1994**, 98, 5552–5556.
- (5) Solbrand, A.; Södergren, S.; Lindström, H.; Rensmo, H.; Hagfeldt, A.; Lindquist, S.-E. *J. Phys. Chem. B* **1997**, 101, 2514–18.
- (6) Enright, B.; Fitzmaurice, D. *J. Phys. Chem.* **1996**, 100, 1027–1035.
- (7) O'Regan, B.; Moser, J.; Anderson, M.; Grätzel, M. *J. Phys. Chem.* **1990**, 94, 8720.
- (8) Cao, F.; Oskam, G.; Meyer, G.; Searson, P. *J. Phys. Chem.* **1996**, 100, 17021–17027.
- (9) Cao, F.; Oskam, G.; Searson, P. *J. Phys. Chem.* **1995**, 99, 17071–17073.
- (10) Huang, S. Y.; Schlitchthörl, G.; Nozik, A. J.; Grätzel, M.; Frank, A. J. *J. Phys. Chem. B* **1997**, 101, 2576–2582.
- (11) Kebede, Z.; Lindquist, S.-E. *Sol. Energy Mater.* **1998**, 51, 291–303.
- (12) Zaban, A.; Meier, A.; Gregg, B. *J. Phys. Chem. B* **1997**, 101, 7985.
- (13) Hoyer, P.; Weller, H. *J. Phys. Chem.* **1995**, 99, 14096–14100.
- (14) Hoyer, P.; Eichberger, R.; Weller, H. *Ber. Bunsen-Ges. Phys. Chem.* **1993**, 97, 630.
- (15) Schwarzburg, K.; Willig, F. *Appl. Phys. Lett.* **1991**, 58, 2520–2522.
- (16) Schwarzburg, K.; Willig, F. *J. Phys. Chem. B* **1997**, 101, 7985.
- (17) de Jongh, P. E.; Vanmaekelbergh, D. *Phys. Rev. Lett.* **1996**, 77, 3427–3430.
- (18) de Jongh, P. E.; Vanmaekelbergh, D. *J. Phys. Chem.* **1997**, 101, 2716–2722.
- (19) Könenkamp, R.; Henniger, R.; Hoyer, P. *J. Phys. Chem.* **1993**, 97, 7328–7330.
- (20) Björkstén, U. On the Photoelectrochemistry of Nanocrystalline Porous Semiconducting Metaloxide Electrodes. Thesis No. 1345, EPFL, Lausanne, Switzerland, 1995.
- (21) Hagfeldt, A. *Sol. Energy Mater.* **1995**, 38, 339–341.
- (22) Hagfeldt, A.; Björkstén, U.; Lindquist, S.-E. *Sol. Energy Mater. Sol. Cells* **1992**, 27, 293.
- (23) Solbrand, A.; Keis, K.; Södergren, S.; Lindström, H.; Rensmo, H.; Hagfeldt, A.; Lindquist, S.-E. Manuscript in preparation.
- (24) Nazeruddin, M. K.; Kay, A.; Rodicio, I.; Humphry, B. R.; Mueller, E.; Liska, P.; Vlachopoulos, N.; Grätzel, M. *J. Am. Chem. Soc.* **1993**, 115, 6382–90.
- (25) Lindström, H.; Rensmo, H.; Södergren, S.; Solbrand, A.; Lindquist, S.-E. *J. Phys. Chem.* **1996**, 100, 3084–3088.
- (26) Lindström, H.; Södergren, S.; Solbrand, A.; Rensmo, H.; Hjelm, J.; Hagfeldt, A.; Lindquist, S.-E. *J. Phys. Chem.* **1997**, 101, 7710–7716.